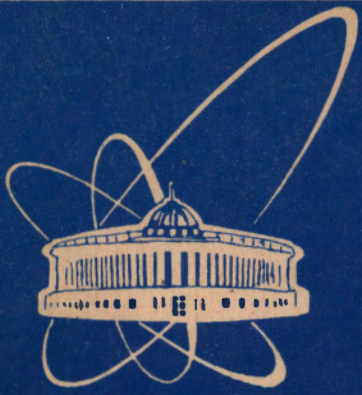

ОБЪЕДИНЕННЫЙ
ИНСТИТУТ
ЯДЕРНЫХ
ИССЛЕДОВАНИЙ

Дубна

E9-96-497

A.S.Artiomov

EXPERIMENTAL STUDY OF H^- ION DETACHMENT ON THIN GAS TARGETS

Submitted to «Nuclear Instruments and Methods B»

1996

INTRODUCTION

To solve a number of applied and fundamental problems by means of accelerator, beams of the negative hydrogen ions are often used at the present time, see, for example, refs.[1-9]. Peculiarities of the H^- ion atomic structure allows one to use a charge-exchanging method to control effectively a fast particle flux [10] in combination with operative and practically nonperturbative diagnostics of the beam using H^o atoms or electrons [11-16]. These information transmitters are produced as a result of detachment of negligible part of the ions on the thin target probing the beam. Maximum accuracy of the coincidence of distributions of the H^- ions and of the particles used for diagnostics in the beam on the angle ($G_{o,e}$, where the bottom "o" or "e" indices correspond to the H^o atoms or electrons, respectively) and relative energy ($\Delta E_{o,e}/E_{o,e}$, where $E_{o,e}$ is the most probable energy of the particle, $E_o = E_{H-}$, $E_e = m_e E_{H-}/M_{H-}$, E_{H-} is the ion energy, m_e and M_{H-} is the electron or ion mass, respectively) is determined by the value and nature of the perturbation the particles acquire in elementary acts of their production. A differential cross section of this process is the most sensitive test of theoretical models describing this interaction.

The results of the experimental study of the H^o atom production as a result of H^- ion detachment on thin gas targets in the energy range of $E_{H-} = 10 \div 300$ keV, are presented in this paper. This energy range is characterized by the beginning of the Born approximation in any theory of the ion detachment, where a good agreement of the predicted distributions and the experiment is the most important. Within the framework of this approach, some peculiarities in the functional dependence of differential cross section of the H^o atom production are not expected at a subsequent growth of the H^- ion energy, and the predicted values of their spread out on the angle and the relative energy, are proportional to $\sqrt{m_e I_e / M_{H-} E_{H-}}$, where I_e is the electron affinity (for H^- ion $I_e = 0.75$ eV). Taking into account the expected angles of the hydrogen atoms and known difficulties in formation of sufficiently intensive thread-like ion beams with a very small angular dispersion (see, for example, [17]), these experiments were realized by means of ribbon-like beams of the H^- ions [18]. In this case small geometrical and angular sizes of the beam at a working coordinate, in combination with a necessary integral intensity of the ion flux and a negligible role of the space charge, are achieved by using a large geometrical size of the beam on the other coor-

dinate. Angular distributions of H^o atoms are measured in this geometry of the experiment by scanning their flux parallel to the ion beam plane at a drift distance (Z_s) by means of a slitting detector or using a multichannel coordinate-sensitive detector. Taking into account a ribbon-like geometry of the experiment in the analysis of the detected distributions, this paper presents the obtained angular distributions of the H^o atoms in elementary acts of the H^- ion detachment on various gas targets, as well as the character of this interaction and the obtained dependence of G_o value versus the ion energy.

1. INFLUENCE OF THE RIBBON-LIKE GEOMETRY OF THE EXPERIMENT WHILE MEASURING PARTICLE ANGULAR DISTRIBUTIONS.

Numerical simulation of detected $I_s(\theta_s)$ distributions at the ribbon-like geometry of the experiment (fig.1) has shown their difference from the true one $I(\theta)$ in elementary acts of interaction [19-21]. As an example,

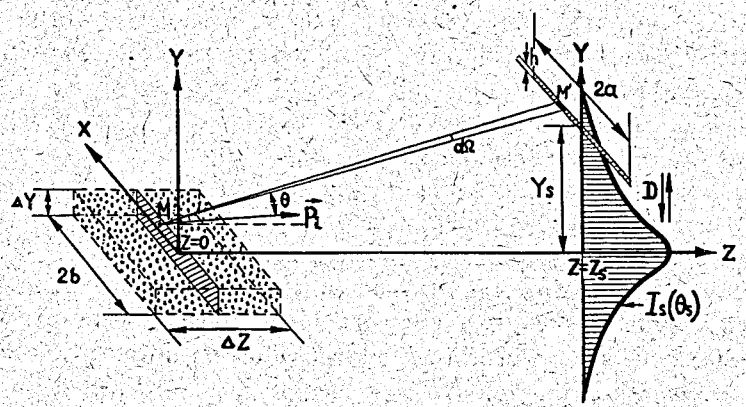

Fig.1. The setup of the experiment on interaction of a ribbon-like beam with the target by using a slitted system of secondary particle detection.

to analyze the character and value of its difference, three possibilities of distributions $I(\theta) = C\exp[-(\theta/G)^2]$ (Gaussian distribution) and $C[1 + (\theta/G)^2]^{-\xi}$ for $\xi = 1,\ 3/2$ (C is the normalized factor), are considered. As experiments have shown [18,22,23], for the thin ribbon-like beams of ions with the electron structure, a small angular disperse and a negligible

role of the space charge, the intensity distribution density in the area of a space localized target ($Z \approx 0,\ \Delta Z \ll Z_s$) can be represented as $f(X,Y) = \Phi(Y)\cdot\Psi(X)$, where $\Phi(Y) = \exp(-Y^2/2\sigma_Y^2)$, value of σ_Y is determined by size ΔY of a slit forming the beam and $\Psi(X) \approx const$ within the beam with a fast decreasing to zero at its boundaries ($X = \pm b$). In this case, for a homogeneous target and $(a,b) \ll Z_s$ ($2a$ is the length of a slit detector) it is not difficult to obtain:

$$I_s(\theta_s) = C\int_{\tilde{Y}} \exp\left(-\frac{Y^2}{2\sigma_Y^2}\right)dY\int_{-b}^{b} dX\int_{-a}^{a} I(\theta)dX'; \qquad (1)$$

where $\theta_s = Y_s/Z_s$, Y_s is the displacement of an infinitely narrow detector in the direction perpendicular to the beam plane, $\theta^2 = [(X' - \alpha X)/Z_s]^2 + [(Y_s - \mu Y)/Z_s]^2$; α and μ are the discrepancy in X and Y coordinate, respectively, of incident particles onto the target ($X_{|Z=Z_s} = \alpha X_{|Z=0}$, $Y_{|Z=Z_s} = \mu Y_{|Z=0}$). For the simplest dependence of $I(\theta)_{|1} = C\exp[-(\theta/G)^2]$

$$I_s(\theta_s)_{|1} = C\cdot\exp\left[-\frac{\theta_s^2}{2\left(\mu^2\sigma_Y^2/Z_s^2 + \sigma_\theta^2\right)}\right]; \qquad (2)$$

independent of values of α, a and b, where $\sigma_\theta = G/\sqrt{2}$. For the second and third possibilities of $I(\theta)_{|\xi}$ distribution with $\xi = 1$ and $3/2$, the following expression (1) is obtained

$$I_s(J_s)_{|\xi=1} = C\int_{\tilde{Y}} \exp\left[-\left(\frac{\tilde{Y}}{R}\right)^2\right]\cdot\left[1 + (J_s - \tilde{Y})^2\right]^{-1/2}\times$$
$$\times\left\{2(A+\alpha B)\cdot\arctan\left[\frac{(A+\alpha B)\cdot}{\sqrt{1+(J_s'-\tilde{Y})^2}}\right] -\right.$$
$$-2(A-\alpha B)\cdot\arctan\left[\frac{(A-\alpha B)}{\sqrt{1+(J_s-\tilde{Y})^2}}\right] -$$
$$\left.-\sqrt{1+(J_s-\tilde{Y})^2}\cdot\ln\left[1+\frac{4\alpha\cdot A\cdot B}{1+(J_s-\tilde{Y})^2+(A-\alpha B)^2}\right]\right\}d\tilde{Y}; \qquad (3)$$

$$I_s(J_s)_{|\xi=3/2} = C\int_{\tilde{Y}} \exp\left[-\left(\frac{\tilde{Y}}{R}\right)^2\right]\cdot\left[1 + (J_s - \tilde{Y})^2\right]^{-1}\times$$

$$\times\left\{\sqrt{1+(J_s-\tilde{Y})^2+(A+\alpha B)^2}-\sqrt{1+(J_s-\tilde{Y})^2+(A-\alpha B)^2}\right\}d\tilde{Y}; \quad (4)$$

where $J_s = \theta_s/G$, $\tilde{Y} = \mu Y/(2Z_sG)$ and $A = a/(Z_sG)$, $B = b/(Z_sG)$, $R = \sqrt{2}\mu\sigma_Y/(Z_sG)$ are dimensionless parameters of the experiment. For the geometry with $(A, \alpha B) \gg 1$, the multipliers in braces of expressions (3) and (4) are practically constant and

$$I_s(J_s)_{|\xi=1} = C\int_{\tilde{Y}} \exp\left[-\left(\frac{\tilde{Y}}{R}\right)^2\right]\cdot\left[1+(J_s-\tilde{Y})^2\right]^{-1/2}d\tilde{Y}; \quad (5)$$

$$I_s(J_s)_{|\xi=3/2} = C\int_{\tilde{Y}} \exp\left[-\left(\frac{\tilde{Y}}{R}\right)^2\right]\cdot\left[1+(J_s-\tilde{Y})^2\right]^{-1}d\tilde{Y}. \quad (6)$$

In this case, for sufficiently thin beams with a small, relatively to G, angular disperse in Y coordinate, the expressions (5) and (6) follow to functional dependences

$$I_s(J_s)_{|\xi=1} = \frac{C}{\sqrt{1+J_s^2}}; \qquad I_s(J_s)_{|\xi=3/2} = \frac{C}{1+J_s^2}; \quad (7)$$

which are different on $I(\theta)_{|\xi=1,3/2}$. For some intermediate values of parameters R, A and B, the results of calculations by using (3) and (4), are presented in fig.2. The presented results have shown that influence of the ribbon-like geometry of experiment depends on the functional view of $I(\theta)$. When the parameter ξ in $I(\theta)_{|\xi}$ grows, this influence decreases and disappears completely in the limit of $I(\theta)_{|1}$.

Usually the geometry of the experiment installation (here values of a, b, σ_Y and Z_s) is fixed. So, for constant functional dependence $I(\theta)$, the value G and consequently the values of parameters A, αB and R are changed when the energy of incidencing particles changes. As a result the values of systematic errors of measurements of particle angular distribution, connected with the ribbon-like geometry of the experiment, will also depend on energy. Therefore, in dependence on measuring parameter of distribution $I(\theta)$ it is necessary to find the corresponding algorithm of the experimental data analysis by numerical simulation and successive approach of calculated distribution $I_s(\theta_s)$ to the measured one. In accordance with the results presented in fig. 2c,d for the fixed geometry of the experiment and equal values of $\theta_{1/2}$, a shape of the numerical angular

distribution is sufficiently sensitive to the change of $I(\theta)$. As an example of a chosen algorithm, fig.3 shows a number of curves to determine a half-width at a half-maximum (HWHM) of $I(\theta)_{|\xi}$ with $\xi = 1$ and $3/2$ by means of experimental dependences $I_s(\theta_s)$ in geometry of ref.[18] (a= 5 мм, b= 2 мм, $Z_s = 10^4$ мм, $\alpha \approx 2$, $\mu \approx 3 \div 6$, $\sigma_Y = 2\cdot 10^{-2}$ мм). In this case the value of $K = \theta_{s1/2}/\theta_{1/2}$ ($\theta_{s1/2}$ and $\theta_{1/2}$ are HWHM of the measured and real distributions, respectively) characterizes the value of

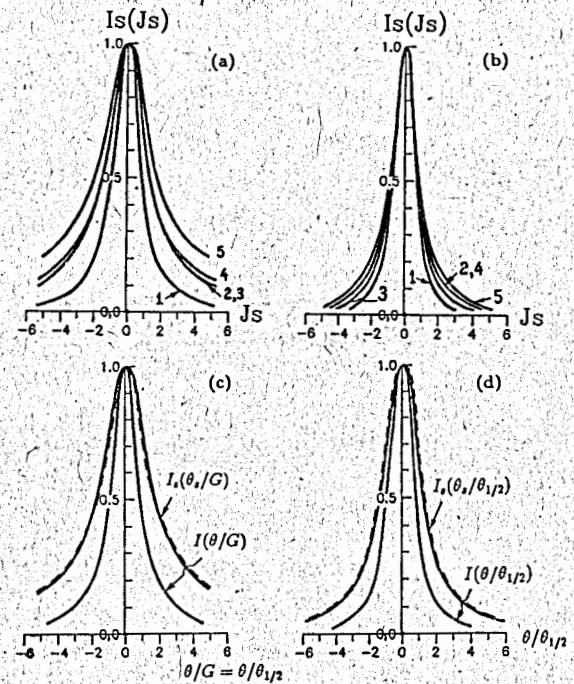

Fig.2. Numerical angular distributons $I_s(J_s)$ for dependences $I(\theta)_{|\xi}$ with ξ= 1 (a,c) and ξ= 3/2 (b,d) and various parameters of R, A and B.
- - - approximation of $I_s(\theta_s)$ by the dependence of $[1+(\theta_s/G_s)^2]^{-\nu}$.
(a,b) - $R = 0.12$; $\alpha = 2$; **1** $\rightarrow$ A = 0.15, B = 0.1;
2 $\rightarrow$ A = 5, B = 0.1; **3** $\rightarrow$ A = 0.15, B = 2; **4** $\rightarrow$ A = 5, B = 2;
5 $\rightarrow$ A = 5, B = 20.
(c,d) - equal half-widths at half-maximum of distributions $I(\theta)_{|\xi}$ ($\theta_{1/2|\xi=1} = \theta_{1/2|\xi=3/2}$, $\theta_{1/2|\xi=1} = G_{|\xi=1}$, $\theta_{1/2|\xi=3/2} = 0.766\cdot G_{|\xi=3/2}$) and
$R = 0.4$, $A = 16.7$, $\alpha B = 13.4$, $\nu = 0.8$ (c);
$R = 0.31$, $A = 12.8$, $\alpha B = 10.3$, $\nu = 1$ (d).

the systematic error influence of the geometry of the experiment on its result. According to the results of numerical simulation, for fractional values of the beam discrepancy, the values of K are determined taking into account a linear dependence between the nearest integers μ [19]. It is necessary to mention the neglected influence of the beam discrepancy in X coordinate on the $I_s(\theta_s)$ distribution and K in a wide range of change of $\alpha = 1 \div 3$ for different fixed values of the other parameters of the experiment geometry. Fig.3 shows that in the area of large measured

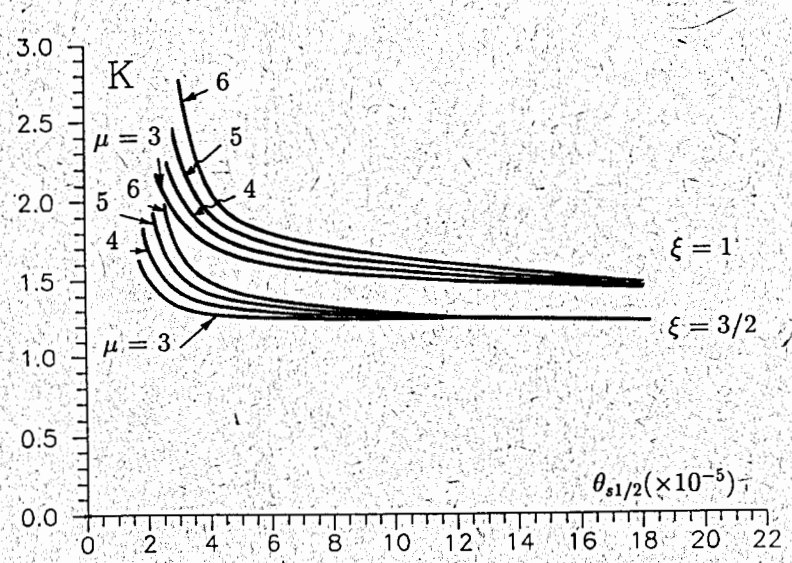

Fig.3. The dependence of K versus $\theta_{s1/2}$[rad] at geometry of experiments in ref.[18] for $\alpha = 2$ and different values of μ and ξ.

angles a connection between the values of $\theta_{s1/2}$ and $\theta_{1/2}$ is defined in principle by parameter ξ and in the end, taking into account the fixed geometry of the experiment, by the shape of distribution $I_s(\theta_s)$. Dependence on μ is displayed noticeably only in the area of sufficiently small measured $\theta_{s1/2}$. A synonymous definition of $I(\theta)$ over experimentally measured dependence of $I_s(\theta_s)$ by using the expression (1), is shown in ref.[21]. When $I_s(\theta_s)$ is well approximated by Gaussian distribution, the

following simple expression can be used to define $\theta_{1/2}$ according to (2)

$$\theta_{1/2} = \sqrt{(\theta_{s1/2})^2 - 2\ln 2 \cdot (\mu \cdot \sigma_Y / Z_s)^2}; \qquad (8)$$

where the values of μ and $\theta_{s1/2}$ are found from detected distributions $I_s(\theta_s)$ of the incident and secondary particles without and after the target, respectively. A comparative analysis has shown, that when parameter ξ in distribution $I(\theta)_{|\xi}$ increases, the difference of values $\theta_{1/2}$, obtained by using the expression (8) and the algorithm analogous to the one presented in fig.3, is decreased. It should be mentioned that the algorithm analogous to the presented one, can be used only in that energy range of the incident particles where parameter ξ or the general shape of distribution $I(\theta)$ can be assumed unchangeable.

2. THE RESULTS OF EXPERIMENTS AND THEIR ANALYSIS.

The experimental study of angular distributions of H^o atoms, created in the result of H^- ion detachment on thin gas targets in the energy range of $E_{H^-} = 10 \div 300$ keV with interval of 10 keV, is given in ref.[18] and realized on the setup shown in fig.1. The needed ribbon-like beam was formed by a number of diaphragms after the ion source, electrostatic accelerator and magnet-separator of particles. The target was formed by means of a gas chamber with the length of $\approx$ 30 cm and feeder for gas injection, slits for noninterceptive beam passage and differential vacuum pumping on both sides. A high time-stability of the initial angular distribution and current of the formed ion beam, large drift distance of particles after the target ($Z_s = 10^3$cm) and good vacuum (a few units per 10^{-8}torr) there allowed one to use a gas target with a sufficiently small and time-stable thickness and also to provide a good angular resolution ($\approx 10^{-6}$rad) of the detector. By means of the magnetic field the particle fluxes are charge separated in space at the end of the drift distance. Passing through the slit D ($10^{-2} \times 10$ mm) the chosen particles were detected by a secondary-electron-multiplier (SEM). A measurement of $I_s(\theta_s)$-distributions was realized by moving the detector in Y-direction with the optimal velocity and by time-registration of an intensive current signal from the SEM. The initial position of the detector slit was established by rotating the detector and choosing such a position when HWHM of the distribution was minimal.

Typical shapes of the obtained distributions of H^o atoms and also H^- ions without and after the target are presented in fig.4. For H^-

ions without the target and for H^o atoms they are well approximated by distributions of $\exp[-\ln 2(\theta_s/\theta_{s1/2})^2]$ and $[1+(\theta_s/\theta_{s1/2})^2]^{-1}$, respectively. Taking into account the parameters of the geometry of this experiment at the measured angles of H^o atoms and results presented in the previous section, the obtained functional distributions of $I_s(\theta_s)$ are complementary

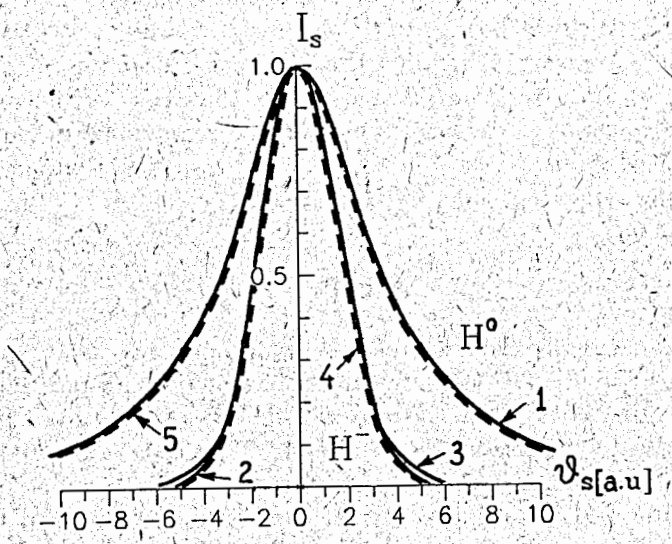

Fig.4. The $I_s(\theta_s)$-distributions (normalized on the amplitude) of flux of H^o atoms (1) and H^- ions without (2) and after (3) the target. Curves 4 and 5 show approximation of distributions by dependences of $\exp[-\ln 2(\theta_s/\theta_{s1/2})^2]$ and $[1+(\theta_s/\theta_{s1/2})^2]^{-1}$, respectively.

with the distribution of $I(\theta) = C[1+(\theta/G)^2]^{-3/2}$ ($G = G_o/1.532$, C is a normalized factor) in elementary acts of H^o atom production. This distribution of $I(\theta)$ is confirmed by the results of ref.[24] on H^- ion detachment at low energy of $E_{H^-} = 500 \div 2000$ eV where the influence of the geometry of the experiment is negligibly small, and also approximates well the theoretical angular distributions of H^o atoms obtained in refs.[25-27] (see fig.5). In accordance with this, to determine the maximum accuracy of the coincidence of angular distributions of H^- ions and H^o atoms versus the energy, the initial experimental data are analyzed by means of the curves presented in fig.3 for $\xi = 3/2$. The dependence of $G_o(E_{H^-})$ obtained this way for thin He, Ar, H_2, N_2, CO_2, Kr and

Xe targets, is shown in fig.6 by points 1 and in the range of the measurement error ±10% is independent of the used target. The theoretical and experimental results of refs.[25-27] and [27,28], respectively, are also presented. For the same functional dependence of $G_o \propto 1/\sqrt{E_{H^-}}$, the results of ref.[28] are essentially higher because the systematic errors of the experiment geometry with circular beams and real angular distributions of H^- ion and H^o atom fluxes, have not been taken into account. That

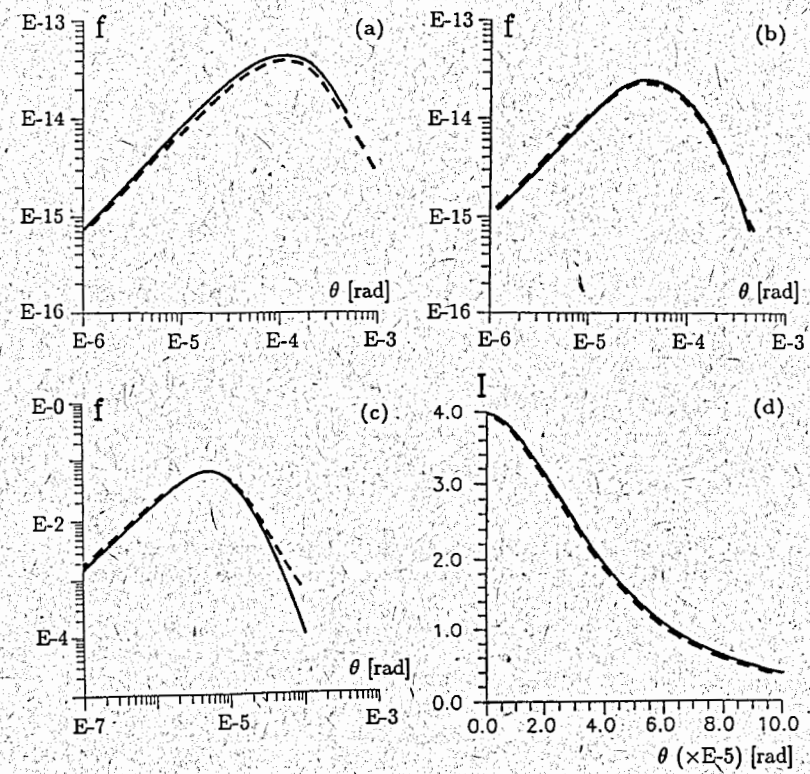

Fig.5. The theoretical angular distributions of $f(\theta) = 2\pi\theta I(\theta)$ and $I(\theta)$[a.u.] of H^o atoms in detachment of H^- ions on various targets
(a) - $H^-(300\ keV) + He$ [25], (b) - $H^-(2\ MeV) + He$ [25],
(c) - $H^-(5\ MeV) + C$ [26], (d) - $H^-(0.71\ MeV) + H$ [27]
and their approximation (- - -) by using
$I(\theta) = C[1+(\theta/G)^2]^{-3/2}$.

is also related to the experimental value of G_o obtained in ref.[27] for the potassium target and the ribbon-like geometry of the experiment at the ion energy of E_{H-}= 5.14 MeV. This difference of the results emphasizes the importance of choosing the proper method to analyze the experimental data in similar experiments. To demonstrate this, fig:6 shows dependence 2 ($G_o \propto E_{H-}^{-0,43}$), which is obtained in ref.[18] in the analysis

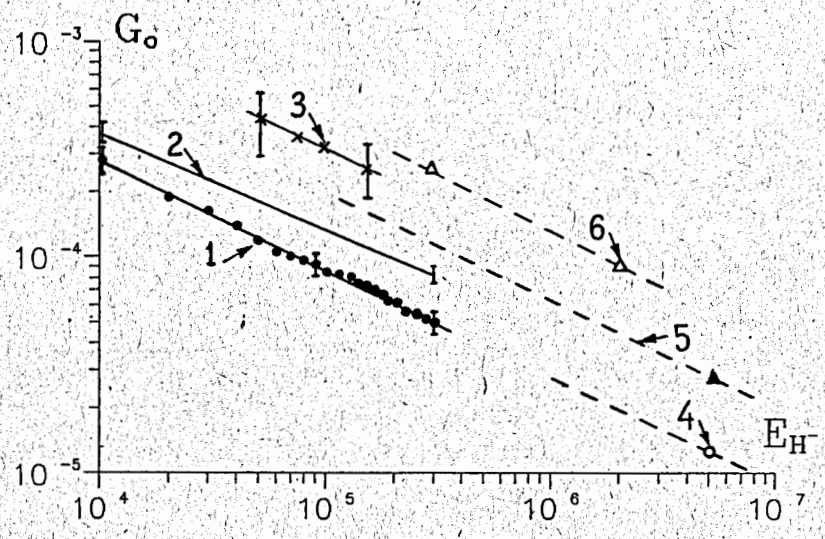

Fig.6. The maximum accuracy of the coincidence of the H^o atom and H^- ion distributions at angle [rad] in the beam for different particle targets versus ion energy [eV].
1 - the experimental results of this work for gas targets of He, Ar, H_2, N_2, CO_2, Kr, Xe and their approximation by dependence of $G_o(E_{H-}) = 3 \cdot 10^{-2}/\sqrt{E_{H-}[eV]}$. **2** - approximation of the experimental results of ref.[18] for the same targets and ion energies ($G_o \propto E_{H-}^{-0,43}$). **3** - the results of measurements of ref.[28] for H_2, He, Ar and Li targets. ▲ - the experimental result of ref.[27] for the potassium target. **4, 5, 6** - the teoretical results of refs.[26], [27] (for unpolarized targets) and [25], respectively (independent of the type of gaseous targets).

of the same experimental data as for dependence 1 by means of the simplest formula (8), which does not take into account the ribbon-like geometry of the experiment and the angular distribution of particles. It is necessary to stress that within the range of the measurement errors, the

obtained results of $G_o(E_{H-})$ are practically independent of thickness of the used gas targets up to the value corresponding to the maximum of $H^- \rightarrow H^o$ detachment. Herewith only shape of the distributions changes somewhat at $\theta > \theta_{1/2}$ (values of $I(\theta)$ grow when the target thickness is increased).

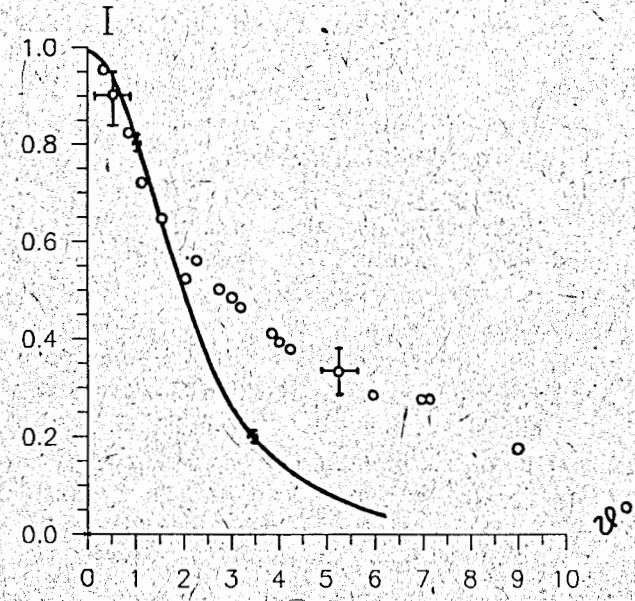

Fig.7. The angular distributions (normalized on the amplitude) of electrons and H^o atoms in elementary acts of H^- ion detachment at the energy of 500 keV and Ar target.
o - the results of measurements for electrons presented in ref.[29].
— - distribution $I(\theta)_{|\xi=3/2}$ for H^o atoms broadened by M_i/m_e times corresponding to the given experimental results.

A good agreement of the obtained experimental results with theory (see 1 and 4 in fig.6) allows one to use the dependence of $G_o(E_{H-}) = 3 \cdot 10^{-2}/\sqrt{E_{H-}[eV]}$ to estimate the accuracy of determination of the H^- ion angular distribution in the beam by means of H^o atoms at the higher energy area of $E_{H-} > 300$ keV. Taking into account the correlation between the half-maximum widths of H^o atom distributions at the energy and angle $\Delta E_o/E_o = (2 \div 2.5) \cdot G_o$, where the smaller value of the proportionality coefficient corresponds to kinematics of the two-particle de-

struction of a particle and the bigger one is estimated from theoretical distributions of ref.[26], the obtained dependence of $G_o(E_{H-})$ can be used for accuracy estimation of the coincidence of the particle distribution on the energy. Curves 2 and 3 in fig.4 show a negligibly small influence of a thin probing particle target on the flux of undetached ions.

A comparison of the H^o atom and electron distributions allows one to represent a character of interaction in detachment of such a weak-connected system as H^- ion. Fig.7 shows the electron production probability normalized at maximum values and various angles θ in the laboratory frame, which was measured in ref.[29] at ion energy of $E_{H-} = 500$ keV and Ar target. The H^o atom distribution $I(\theta)_{|\xi=3/2}$ with the half-maximum width determined by approximation of the results 1 in fig.6 broadened by M_i/m_e times that is also shown in fig.7. The maximum angle of the presented distributions corresponds to the boundary of the H^o atom detection in the experiment. A small (in the limits of measurement errors) difference of the distributions at the angles of $\theta \leq \theta_{1/2}$ indicates a dominating two-stage mechanism of H^- ion detachment at this energy and large impact parameters of ion interaction with a target particle whose influence displays only at the initial stage of the ion detachment. As a result of this interaction stage, the ion transforms into the excited quasiparticle with its following two-particle destruction into hydrogen atom and electron. At smaller impact parameters corresponding to the larger angles and smaller differential cross sections, this mechanism of interaction is disturbed and a contribution of separate influence of the third body (target particle) on ion components (H^o atom and electron) is increased. Herewith the internal degrees of freedom of atom (its excitation is occurs) or H^- ion can be affected with the following destruction of the last one through autoresonance states [30]. Other mechanisms of detachment (quasimolecular and resonant), which are noted, for example, in ref.[31], display only at sufficiently small velocities of negative ions $V_i \leq 10^8$ cm/s, which correspond to the H^- ion energy of $E_{H-} \leq 5$ keV.

References

1. Burgerjon J.J. - Nucl. Instr. and Meth. B, 1985, V.10/11, Pt.2, P.951-956.
2. Gullickson R.L. - Nucl. Instr. and Meth. B, 1987, V.24/25, P.730-735.
3. Mc Kenzie-Wilson R.B. - Nucl. Instr. and Meth. B, 1991, V.56/57, Pt.2, P.987-990.

4. Bowman C.D., Arthur E.D., Lisowski P.W. et al. - Nucl. Instr. and Meth. A, 1992, V.320, Nos.1/2, P.336.
5. Isler R.C. - Plasma Phys. and Contr. Fusion, 1994, V.36, No.2, P.171-208.
6. Junzo Ishikava, Hiroshi Tsuji et al. - Nucl. Instr. and Meth. B, 1995, V.96, Nos.1/2, P.7-12.
7. Stewart J.E., Bryant H.C. et al. - Phys. Rev. A, 1988, V.38, No.11, P.5628-5638.
8. Bryant H.C., Donahue J.B. et al. - Nucl. Instr. and Meth. B, 1991, V.56/57, Pt.1, P.205-210.
9. Harris P.G., Bryant H.C. et al. - Phys. Rev. A, 1990, V.42, No.11, P.6443-6445.
10. Dimov G.I., Dudnikov V.G. - Fizika plazmy, 1978, V.4, No.3, P.692-703 (in russ.).
11. Stephen L. Kramer, D. Read Moffett - IEEE Trans. on Nucl. Science, 1981, V.NS-28, No.3, P.2174-2176.
12. Cottingame W.B., Boicourt G.P., Cortez J.H. et al. - IEEE Trans. on Nucl. Science, 1985, V.NS-32, No.5, P.1871-1873.
13. Artiomov A.S., Vaganov N.G. et al. - IEEE Part. Accel. Conf., San Francisco, CA, May 6-9, 1991, P.1573-1575.
14. Connolly R.C., Johnson K.F., Sandoval D.P., Yuan - Nucl. Instr. and Meth. A, 1992, V.312, No.3, P.415-419.
15. Artiomov A.S. - Proc. 6th Intern. Symp. on Product. and Neutr. of Negative Ions and Beams, Upton, NU, 1992, P.579-585.
16. Artiomov A.S. - ibid, P.586-591.
17. Armstrong D.D., Wegner H.E. - Rev. Sci. Instrum., 1971, V.42, No.1, P.40-44.
18. Artiomov A.S., Arutinov V.N., Baturin V.A. et al. - (1977-1978)-year SPTI reports, Sukhumi (in russ.).
19. Artiomov A.S. - SPTI report, Sukhumi, 1978, P.1-110 (in russ.).

20. Artiomov A.S., Levkovich N.A. - Preprint SPTI-90-12, Moscow, TsNIIatominform, 1990 (in russ.).

21. Artiomov A.S. - Preprint JINR P13-96-54, Dubna, 1996 (in russ.).

22. Vedmanov G.D., Kozlov V.P. et al. - Pribory i Tekhn. Eksperim., 1989, No.2, P.47-50 (in russ.).

23. Radchenko V.I. - Zh. Eksp. Teor. Fiz., 1993, V.103, No.1, P.40-49 (in russ.).

24. Van Der Leeuw P.E., Tip A. et al. - Chemical Physics, 1986, V.101, No.2, P.183-199.

25. Lee Y.T., Chen J.C.Y. - Phys. Rev. A, 1979, V.19, No.2, P.526-533.

26. Johnstone J.A. - Nucl. Instr. and Meth. B, 1990, V.52, No.1, P.1-8.

27. Radchenko V.I. - Zh. Eksp. Teor. Fiz., 1994, V.105, No.4, P.834-852 (in russ.).

28. Dyachkov V.A., Zinenko V.I., Kazantsev G.V. - Zh. Tekhn. Fiz., 1977, V.47, No.2, P.416-420 (in russ.).

29. Duncan M.M., Menendez M.G. - Phys. Rev. A, 1977, V.16, No.5, P.1799-1804.

30. Buckman Stephen J., Clark Charles W. - Rev. Mod. Phys., 1994, V.66, No.2, P.539-655.

31. Ilin P.I., Sakharov V.I., Serenkov I.T. - Fiz. Elektr. i Atomn. Stolkn., 1989, No.11, P.142-150 (in russ.).

Received by Publishing Department
on December 27, 1996.